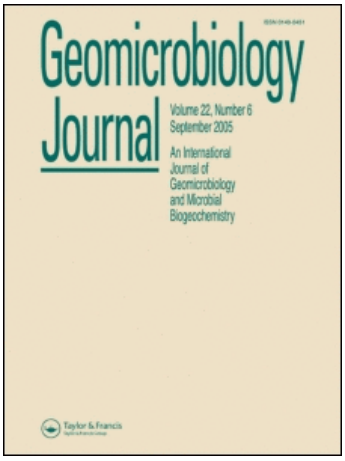

Geomicrobiology Journal
Publication details, including instructions for authors and subscription information:
http://www.informaworld.com/smpp/title~content=t713722957

High Resolution Analysis of Contaminated Aquifer Sediments and Groundwater—What Can be Learned in Terms of Natural Attenuation?

Bettina Anneser[a]; Giovanni Pilloni[a]; Anne Bayer[a]; Tillmann Lueders[a]; Christian Griebler[a]; Florian Einsiedl[b]; Lars Richters[c]
[a] Institute of Groundwater Ecology, Helmholtz Zentrum München, Neuherberg, Germany [b] Department of Environmental Engineering, Technical University of Denmark, Kgs., Lyngby, Denmark [c] Stadtwerke Düsseldorf AG, Duesseldorf, Germany

Online publication date: 17 March 2010

To cite this Article Anneser, Bettina , Pilloni, Giovanni , Bayer, Anne , Lueders, Tillmann , Griebler, Christian , Einsiedl, Florian and Richters, Lars(2010) 'High Resolution Analysis of Contaminated Aquifer Sediments and Groundwater—What Can be Learned in Terms of Natural Attenuation?', Geomicrobiology Journal, 27: 2, 130 — 142
To link to this Article: DOI: 10.1080/01490450903456723
URL: http://dx.doi.org/10.1080/01490450903456723

Geomicrobiology Journal, 27:130–142, 2010

ISSN: 0149-0451 print / 1521-0529 online
DOI: 10.1080/01490450903456723

Taylor & Francis
Taylor & Francis Group

High Resolution Analysis of Contaminated Aquifer Sediments and Groundwater—What Can be Learned in Terms of Natural Attenuation?

Bettina Anneser,[1] Giovanni Pilloni,[1] Anne Bayer,[1] Tillmann Lueders,[1] Christian Griebler,[1] Florian Einsiedl,[2] and Lars Richters[3]

[1]*Institute of Groundwater Ecology, Helmholtz Zentrum München, Neuherberg, Germany*
[2]*Department of Environmental Engineering, Technical University of Denmark, Kgs. Lyngby, Denmark*
[3]*Stadtwerke Düsseldorf AG, Duesseldorf, Germany*

High-resolution depth-resolved monitoring was applied to groundwater and sediments samples in a tar oil contaminated aquifer. Today, it is not fully clear, whether groundwater-based lines of evidence are always sufficient to adequately assess natural attenuation (NA) potentials and processes going on *in situ*. Our data unveiled small-scale heterogeneities, steep physical-chemical and microbial gradients, as well as hot spots of contaminants and biodegradation in the supposedly homogeneous sandy aquifer. The comparison of basic geochemical data revealed a fairly good agreement between sediment and groundwater samples. Nevertheless, a comprehensive understanding of both BTEX and PAH distribution, as well as redox processes involving insoluble electron acceptors, i.e., iron reduction, clearly asks for consideration of both, sediment and groundwater analysis. A thin BTEX plume right below the groundwater table was visible only in groundwater, while significant amounts of PAHs were present in sediments from deeper zones of the aquifer. Indications for sulfate reduction as a dominant process involved in BTEX degradation were largely obtained from groundwater, while the role of iron reduction in degradation and possible sulfide oxidation at the capillary fringe and the upper BTEX plume fringe, as well as in deeper PAH-contaminated zones was evident from sediments. Moreover, sediment analyses were essential to meaningfully recover cell abundances, distribution, activity and composition of the bacterial community. Sediments harbored >97.7% of bacterial cells and displayed enzyme activities 5 to 6 orders of magnitude higher than groundwater samples. Bacterial community T-RFLP fingerprints revealed important distinctions, but also similarities in depth-resolved microbial community distribution in sediments and water. An apparently highly specialized degrader population was found to dominate the lower BTEX plume fringe. However, even though sediment data seemed to comprise most community information found also in groundwater, this relation did not apply *vice versa*. In summary, our results show that groundwater sampled at an appropriate scale may contain sufficient information to identify and localize dominant redox reactions, but clearly fails to unravel natural attenuation potentials. This clearly emphasizes the importance of both groundwater and sediment samples for truly assessing natural attenuation potentials and activities at organically contaminated aquifers.

Keywords aquifers, geochemistry, groundwater, microbial communities, natural attenuation, small-scale heterogeneity

INTRODUCTION

Contaminations with complex mixtures of petroleum hydrocarbons are known to exhibit a long-term persistence in soils and aquifers, and may be detectable even after thousands of years (Eberhardt and Grathwohl 2002). In many cases, a complete remediation of contaminations fails, despite application of vigorous physical-technical remediation (e.g., air sparging, thermal treatment or pump and treat techniques) or biostimulation approaches. The monitoring of natural attenuation (NA) is therefore often chosen as a cost- and labour-efficient strategy to follow the transport and fate of pollutants in subsurface environments (Bamforth and Singleton 2005). Consequently, there's a growing interest to predict the spread and development of contaminant plumes and to understand intrinsic degradation behaviour. NA is controlled by a complex interplay of physical, chemical and biological reactions, which are in turn affected by sediment-porewater interactions (Haack and Bekins 2000; McGuire et al. 2000).

The distribution and transport of contaminants in groundwater, the distribution and structure of microbial degrader populations, as well as actual biodegradation activities are at least partially determined by sediment and groundwater characteristics. The monitoring of NA at a given site usually involves the investigation of a limited set of groundwater parameters (i.e., contaminants, redox species), but rarely also considers geochemical and microbiological analyses of sediments, or both groundwater and sediments (Bekins et al. 2001; Lehman et al. 2001). For aquifer microbial populations, however,

Received 15 April 2009; accepted 5 October 2009.
Address correspondence to Christian Griebler, Helmholtz Zentrum München, Institute of Groundwater Ecology, Ingolstaedter Landstrasse 1, D-85764 Neuherberg, Germany. E-mail: christian.griebler@helmholtz-muenchen.de

it is known that the major part occurs associated to sediments (e.g., Hazen et al. 1991; Albrechtsen and Winding 1992; Alfreider et al. 1997; Griebler et al. 2002), and activities are often found higher for attached cells (e.g., Holm 1992; Madsen and Ghiorse 1993; Albrechtsen and Christensen 1994).

Previous studies have also revealed that considerable discrepancy in microbial community composition and biodegradation potential can prevail between sediment and groundwater samples of the same location (Lehman et al. 2001; Röling et al. 2001; Brad et al. 2008). It is therefore not fully clear, whether monitoring of groundwater is sufficient to adequately assess *in situ* NA processes and potentials at a specific site. It is frequently hypothesized that most degradation processes in aquifers are catalyzed by attached microbial populations (Kölbel-Boelke and Hirsch 1989; Röling et al. 2001; Lehman and O'Connell 2002; Brad et al. 2008).

However, respective data sets comparing NA process information obtainable in sediment vs. water samples taken at a given site are extremely rare. Due to the considerable efforts associated with borehole drilling and installation of multi-level monitoring wells, only a limited number of studies is available where both groundwater and sediment analysis have been conducted in parallel today. Furthermore, the spatial resolution of sampling may often not be sufficient to adequately recover small-scale sediment heterogeneities and the reactive biogeochemical gradient zones at the fringes of contaminant plumes (Cozzarelli et al. 1999; Kao et al. 2001; Anneser et al. 2008a; Brad et al. 2008; Winderl et al. 2008).

In this study, we present a comprehensive data set comparing the biogeochemistry and microbiology of groundwater and sediment samples from a tar oil-contaminated sandy aquifer. Temporally and spatially closely connected sampling allowed a direct comparison of both sediment and groundwater characteristics and enabled us to localize and scrutinize NA potentials. In particular, the distribution of contaminants and redox reaction products in groundwater and sediments was assessed in relation to the abundance, activity, diversity and distribution of bacteria present in different zones of the contaminated aquifer. Important distinctions in the two different data sets were more than evident. While distinct abiotic features may be sufficiently recovered by groundwater monitoring, this study especially points out the importance of sediment matrix-based information for assessing major microbial NA potentials.

MATERIALS AND METHODS

Site Description

The investigated area is a Quaternary sandy aquifer at a former gasworks site in Düsseldorf-Flingern, Germany. Release of tar oil compounds during operation and break-down of the plant resulted in the development of a contaminant plume with concentrations of up to 100 mg L^{-1} of monoaromatic and 10 mg L^{-1} of polycyclic aromatic hydrocarbons (PAHs) dissolved in groundwater. In the course of several remediation actions launched since 1995 the major part of the tar oil phases was removed. Nevertheless, residual amounts still can be detected in sediments and groundwater, forming a hydrocarbon plume of about 200 × 40 m in horizontal dimension. For detailed information on site characteristics see (Eckert 2001; Anneser et al. 2008a, 2008b).

Groundwater Sampling

In February 2006, groundwater was collected from a specially designed high-resolution multi-level well (HR-MLW), which extends from 3 m to 12 m below land surface (bls) and exhibits sampling filter spacings of 2.5 cm, 10 cm and 30 cm. For geochemical analyses, groundwater was sampled at vertical intervals of 2.5–10 cm from 6.38 m (groundwater table) down to 8.1m below land surface (bls) in 100 mL pre-washed narrow neck glass bottles and immediately processed for the analysis of a number of biotic and abiotic parameters, as described below. Water samples for microbial community analyses were sampled from only 5 selected depths down to 9 m bls. Here, water was collected in autoclaved 1 L glass bottles, sealed on site to minimise oxygen exposure, and transported to the lab within 24 h under cooling (<10°C). In the lab, ~750 mL per depth were filtered over 0.22 μm cellulose acetate filters (Corning Inc., NY, USA), which were immediately frozen until DNA extraction. A detailed description of the HR-MLW as well as information on the sampling procedure and the materials and instruments used is given in (Anneser et al. 2008a, 2008b).

Sediment Sampling

One week after sampling groundwater, two boreholes were drilled in a distance of approximately 0.5 m downgradient and, respectively, 1.5 m adjacent to the HR-MLW by means of hollow-stem auger drilling. Sediment liners were obtained in one meter segments down to a depth of 14 m (Liner 1) and 11 m (Liner 2). Right after retrieving the sediment liners they were transferred into an aluminium box and subsampled immediately under argon atmosphere for a selected set of parameters. Sediment sub cores from selected depths were immediately fixed for individual parameter measurements (see below), or frozen on dry ice for subsequent DNA extraction and molecular community analyses (Winderl et al. 2008).

Sample Preparation and Geochemical Analysis

Groundwater collected in 100ml glass bottles was immediately processed for measuring specific conductivity, pH and redox potential as well as for the analysis of dissolved iron and sulfide species, which is described in detail in Anneser et al. (2008a). Total reduced inorganic sulfur was extracted from sediment samples fixed in 20% (w/v) zinc acetate using HCl-Cr(II) solution (1M Cr(II)-HCl in 12M anoxic HCl), according to the protocol of (Ulrich et al. 1997). Under maintenance of anoxic conditions, reduced inorganic sulfur species were converted to hydrogen sulfide during 30 h of intensive shaking at

room temperature. The liberated H_2S was trapped in a 10 % zinc acetate solution and subsequently analyzed analogous to groundwater sulfide measurements (Anneser et al. 2008a).

Groundwater samples dedicated to the analysis of dissolved mono- and polycyclic aromatic hydrocarbons were amended with NaOH (0.1 M final concentration) to stop biological activity. BTEX concentrations were measured via GC-MS by headspace analysis; the less soluble polycyclic aromatic hydrocarbons (PAH) were extracted with cyclohexane and determined by liquid injection analysis. Major anions (SO_4^{2-}, HPO_4^{3-}) and cations were analyzed via ion chromatography (Dionex DC-100, Idstein, Germany). Further details on analytical procedures are given in (Anneser et al. 2008a).

Sediment total organic matter (TOM) was calculated from the loss in weight of dried sediment after combustion of the organic content at 450°C for 4 h. Amorphous, ready available sedimentary iron was extracted in duplicates with 30 mL of 0.5 M HCl from 2 mL of sediment during 24 h of intensive shaking at room temperature (Heron et al. 1994). Likewise, crystalline iron phases were obtained by 5 M HCl extraction over a period of 21 days. The extracted Fe(II) was measured analogous to groundwater samples (Anneser et al. 2008a). Concentrations of ferric iron species were determined after reduction of total iron to Fe(II) using hydroxylamine hydrochloride (HACl; 10% w/w in 1M HCl) as reductant. The amount of HACl-reducible Fe(III) was calculated as the difference of Fe(II) determined in the HCl and HACl extracts (Lovley and Phillips 1987).

PAHs adsorbed to the sediment were extracted with acetone and amended with an internal standard mixture containing deuterated acenaphthene, chrysene, perylene and phenanthrene species (Internal Standards Mix 25, Ehrenstorfer, Augsburg, Germany) at a final concentration of 25 mg L^{-1}. Aromatic hydrocarbons were determined in a GC-MS applying the settings as described in (Winderl et al. 2008).

In situ microbial activity was assessed by determining the enzymatic hydrolysis rates of two fluorogenic substrates, i.e., MUF-P (4-methylumbelliferyl phosphate) and MUF-Glc (4-methylumbelliferyl β-D-glucoside) (Freeman et al. 1995; Hendel and Marxsen 1997). Enzyme assays of both groundwater and sediment samples were performed in 4 mL Supelco glass vials. For each sample, three replicates and one control were prepared. Groundwater was filled immediately after sampling into the vials avoiding headspace. Sediment samples were transferred in aliquots of 1 mL into vials, which have been prefilled with anoxic, low-ionic strength (1:500 dilution) freshwater medium (Widdel and Bak 1992).

The substrates MUF-P or MUF-Glc (both Sigma, Taufkirchen, Germany) were added to a final concentration of 225 μM to groundwater samples and 1 mM to sediment samples, respectively. After incubation at *in situ* temperature (16°C ± 1°C) for 18 h, groundwater samples were stopped by addition of ammonium glycine buffer (pH 10.5) at a ratio of 1:10. Enzyme activity within sediment samples was terminated after 22 h of incubation (16°C ± 1°C) by adding 100 μL of an alkaline solution (2M NaOH/0.4M EDTA) to each sample. Controls for background fluorescence were treated analogously, but inactivated prior to incubation. Fluorescence was determined in a luminescence spectrometer (Aminco Bowman Series 2, Thermo Scientific) at 455 nm emission and 365 nm excitation.

Stable Isotope Analysis of Sulfate

Stable sulfur ($^{34}S/^{32}S$) and oxygen ($^{18}O/^{16}O$) isotope ratios of sulfate dissolved in groundwater were determined from samples collected in 100 mL vessels containing 10 mL of a 20% (w/v) Zn-acetate solution for precipitation of sulfide. Procedures for the recovery of sulfate and details on isotope measurements are described elsewhere in detail (Anneser et al. 2008a).

Determination of Bacterial Cell Numbers

From sediment liners stored at −20°C, 0.5 mL sample aliquots were fixed with 2.5% glutardialdehyde and kept at 4°C until further preparations. After replacement of the glutardialdehyde by 1.5 mL PBS, cells were released from sediment using a swing mill (Retsch, MM 200; 3 min, 20 Hz) and separated from abiotic particles via density gradient centrifugation according to the protocol of Lindahl and Bakken (1995). The layer containing the bulk (about 80%) of bacterial cells was collected and cells were stained with SYBR green I (Molecular Probes, Invitrogen, Karlsruhe, Germany) at a ratio of 1:10,000. Total cell counts were quantified in a flow cytometer (LSR II, Becton Dickinson, Heidelberg, Germany) equipped with a 488 nm and 633 nm laser, using TruCount beads (TruCount Tubes, Becton Dickinson) as internal standard. Instrument settings were as follows: forward scatter (FSC) 350 mV, side scatter (SSC) 300–370 mV, B530 (bandpass filter 350 nm) 500–580 mV. All parameters were collected as logarithmic signals. For minimization of background noise, the threshold was adjusted to 200 mV each for FSC and SSC. Calculations of total bacterial cell numbers were performed as described in Nebe-von-Caron et al. (2000). Loss of cells due to sediment freezing was accounted for applying a correction factor determined from fresh and frozen sediments from a later sampling at the same site (Bayer et al. in prep.).

Bacterial Community Fingerprinting

DNA was extracted from 6 different sediment depths of Liner 1 (6, 6.4, 6.65, 6.9, 7.1, 7.6, 7.8, 8.1, and 9.2 m) and available corresponding groundwater filtrates (6.38, 6.46, 6.83, 7.1, 8.1 and 9.0 m). The extraction protocols used for sediments (∼1 g wet weight) and filters were as previously described (Winderl et al. 2008; Brielmann et al. 2009), using a CTAB extraction buffer (Zhou et al. 1996) modified as follows: 100 mM Tris, 100 mM Na-EDTA, 95 mM Na_2HPO_4, 750 mM NaCl, 1% CTAB, pH 7.80. Extracted DNA was stored frozen (−20°C) until further analyses. Terminal restriction fragment length polymorphism (T-RFLP) analysis of bacterial 16S rRNA gene amplicons was done with primers Ba27f-FAM/907r and *Msp*I digestion as

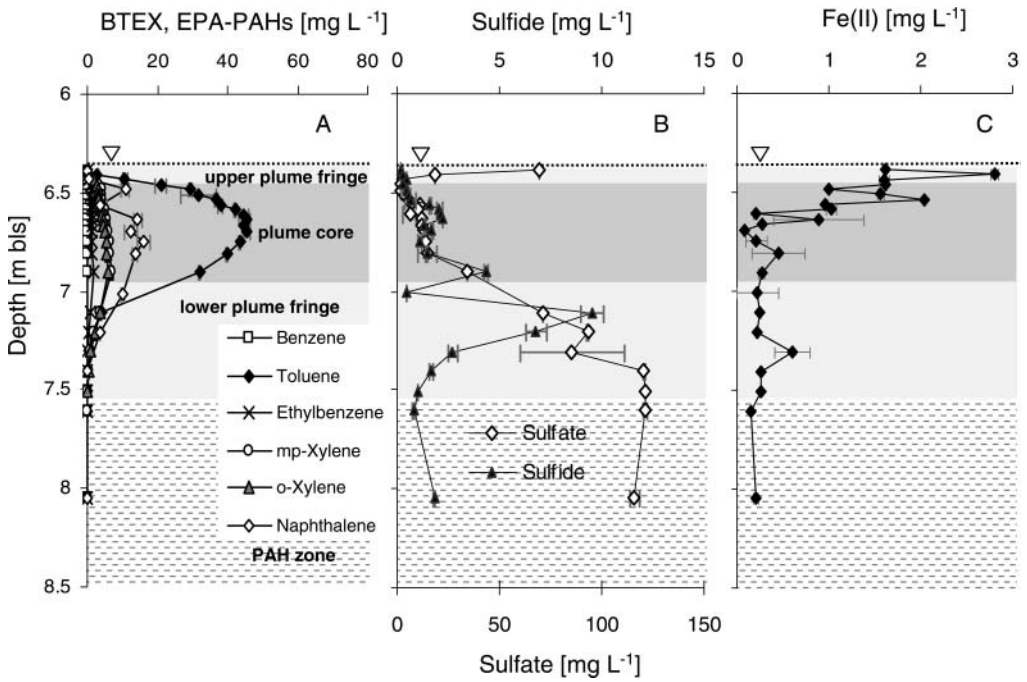

FIG. 1. Small-scale distribution of (A) contaminants, (B) sulfate and sulfide, and (C) ferrous iron in groundwater sampled from the HR-MLW; values represent means of duplicate measurements ± SD.

previously described (Winderl et al. 2008). Data evaluation and principal component analyses (PCA) was performed as reported elsewhere (Lueders and Friedrich 2002; Winderl et al. 2008).

RESULTS

Distribution of Contaminants

The spread of major contaminants (e.g., benzene, toluene, ethylbenzene and xylenes; BTEX) in groundwater of the investigated aquifer section was restricted to a narrow zone stretching from right below the groundwater table (ca. 6.4m bls at time of sampling) to a depth of approximately 8.1 m bls, describing a vertically thin plume with a maximum BTEX concentration of 58 mg L^{-1} at 6.7 m depth (Figure 1A). Toluene constituted the main fraction of monoaromatic hydrocarbons, accounting for about 75% of total BTEX concentrations. For naphthalene, the major dissolved PAH component, a similar depth profile was found with a maximum concentration of 16 mg L^{-1} at 6.75 m bls (Figure 1A). Out of the 16 EPA-PAHs, only acenaphthene and fluorene were further detected in groundwater, with lowest concentrations in the area of the BTEX plume and slightly increased values (<1 mg L^{-1}) further down (>7m bls) (data not shown).

Sediment samples contained no detectable amounts of BTEX, but exhibited distinct peaks for individual PAHs such as naphthalene, acenaphthene and fluorene. In detail, concentration maxima within Liner 1 were found at 6.65 m and 8.8 m bls (Figure 2A). Both maxima were mainly contributed by naphthalene, with the upper peak located directly within the center of the plume, and the lower in an area where no BTEX and only minor concentrations of PAHs, i.e., acenaphthene and fluorene, could be detected in groundwater. Interestingly, no other of the 16 EPA-PAHs were found or, if yet, they were below the detection limits of the respective extraction and analysis protocols (i.e., 20 μg L^{-1} for groundwater and 6.8 μg kg^{-1} wwt for sediments). The distribution patterns of total PAHs within Liner 2 were found to be quite similar to Liner 1 for the upper layers of the saturated zone, yet concentrations of individual components partly differed. Additionally, a PAH-impacted layer that was not present in Liner 1 was detected at 10.2 m bls (Figure 2B), thus pointing at lateral sediment heterogeneities.

Physical-Chemical Conditions and Redox-Specific Parameters

The redox potential (E_h) in groundwater rapidly declined with depth from −20 mV at the uppermost sampling point to a value of −235 mV in the plume center (6.81 m; Table 1). A trend opposite to E_h was observed for pH, starting at a value of 7.07 right below groundwater table and a maximum of 7.46 at 6.81 m bls (Table 1). Likewise, specific conductivity ranging from 1030 to 1215 μS cm^{-1} showed an increasing trend with depth (Table 1). Dissolved inorganic phosphate was available all across the investigated aquifer section, with lowest concentrations of 70 μg L^{-1} at the water table and peak values of up to 2.1 mg L^{-1} in the plume center (Table 1). No nitrate (detection limit of 0.1 mg L^{-1}) could be detected in groundwater at time of sampling. Sulfate, the most important dissolved electron acceptor, was almost absent in the BTEX plume center, yet

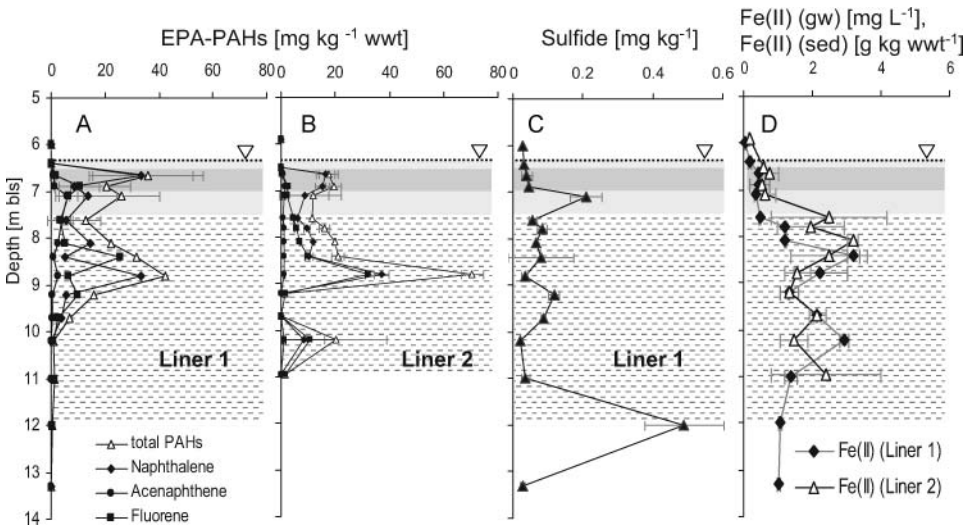

FIG. 2. (A) Vertical distribution of (A, B) contaminants, (C) sulfide, and (D) ferrous iron in sedimentsin relation to BTEX (grey area) and PAH (shaded area) contamination zones, respectively; values represent means of duplicate measurements ± SD.

its availability increased rapidly with declining contaminant concentrations at the upper and lower plume fringe (Figure 1B). At a depth of 7.4 m bls, sulfate leveled off to a concentration of about 120 mg L^{-1}.

Stable isotope values of sulfate, i.e., $^{34}S/^{32}S$ and $^{18}O/^{16}O$, determined for selected depths indicated the occurrence of bacterial sulfate reduction in the contaminated aquifer (Table 1). Concomitant with declining concentrations of organics and increasing sulfate concentrations at the lower plume fringe, distinct peaks of dissolved sulfide were observed, reaching a maximum of almost 10 mg L^{-1} at 7.11 m bls (Figure 1B). Lower amounts of sulfide were detected in the plume core and scarcely any dissolved sulfide was found within the first centimeters beneath the capillary fringe. There, however, elevated concentrations of dissolved Fe(II) were measured, followed by a steep decline until approximately constant concentrations of about 0.3 mg L^{-1} were attained at 6.9 m bls (Figure 1C).

In contrast, ferrous iron extracted from the sediments (0.5M HCl) exhibited lowest concentrations within the BTEX contamination area but exhibited a pronounced increase with depth, reaching concentrations of up to 3.2 g kg^{-1} wwt beneath 8 m bls (Figure 2D). With the exception of local peaks at 10.2 m (Liner 1) and 9.2 m (Liner 2) bls, the recovery of ready extractable Fe(III) from saturated sediments was considerably lower compared to that of Fe(II), i.e., always <1 g kg^{-1} in Liner 1 and, respectively, <2 g kg^{-1} wwt in Liner 2 (data not shown). Only low amounts of crystalline Fe(II) averaging 1 mg kg^{-1} were obtained by extraction with 5M HCl; in contrast, concentrations of Fe(III) released by this harsh extraction exhibited clearly higher values of up to 5.5 g kg^{-1} wwt (data not shown). Total reduced inorganic sulfur extracted from sediment samples of Liner 1 revealed concentrations in the range of 0.02 – 0.5 g sulfide per kg (wwt), with pronounced peaks at 7.1 and 12 m depth (Figure 2C). Unfortunately, no sulfide values are available from Liner

TABLE 1
Hydrogeochemistry and stable isotope ratios of groundwater sampled from the HR-MLW

Depth [m]	pH	Redox [mV]	Specific conductivity [μS cm^{-1}]	HPO_4^2[mg L^{-1}]	SD	$\delta^{34}S$ [‰]	SD	$\delta^{18}O$ [‰]	SD
6.39	7.07	−20	1096			5.5	0.04	2.1	0.18
6.41		−100	1030	0.07					
6.46	7.13	−100	1053	0.54	0.02				
6.56	7.27	−150	1052	2.05	0.18				
6.67	7.4	−190	1081	1.19	0.17				
6.75	7.43	−195	1094	1.07	0.38				
6.81	7.46	−235	1138	1.18		42.4	0.17	15.2	0.04
7.11	7.42	−230		0.44	0.05	25.0	0.20	12.6	0.13
7.41	7.39	−197	1215	0.95	0.12				
8.05	7.43	−229	1166	0.57	0.06	15.9	0.02	11.1	0.11
9.05						12.5	0.02	10.7	0.05

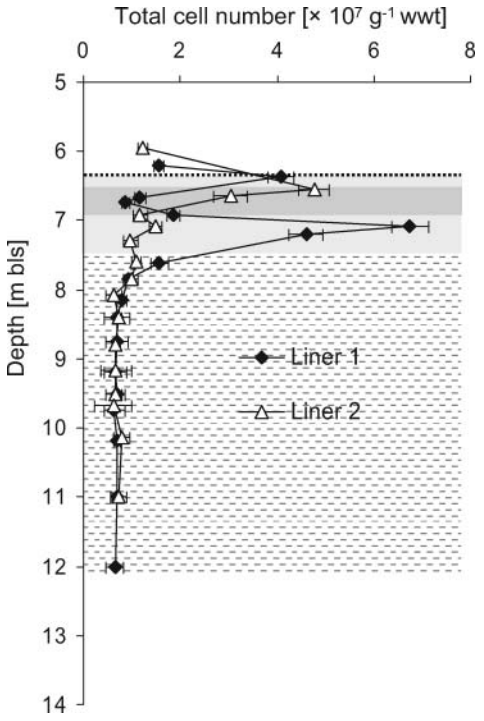

FIG. 3. Total number of bacteria in sediments from Liner 1 and 2 in relation to BTEX- and PAH-contaminated zones; values represent means of triplicate measurements ± SD.

2 sediments. Total organic matter (TOM) content in dried sediments of both liners ranged between 0.2 and 0.6% (dwt), with a mean value of 0.34% in Liner 1 and 0.39% in Liner 2.

Direct Cell Counts and Enzyme Activities

In sediments of Liner 1, bacterial cell counts exhibited two distinct peaks of 4.1×10^7 and 6.8×10^7 cells g^{-1} wwt at the upper and lower fringe of the BTEX plume, separated by a local minimum of 8.8×10^6 cells g^{-1} wwt in the plume center (Figure 3). Background numbers in the less contaminated zone below 8 m bls averaged at 6.8×10^6 cells g^{-1} wwt. In contrast, direct cell counts in sediments of Liner 2 exhibited one dominant peak of 4.8×10^7 cells g^{-1} wwt at the upper plume fringe (Figure 3) and only a less distinct increase of cell number at the lower plume fringe. With depth, cell numbers decreased significantly down to background concentrations of 6.9×10^6 cells g^{-1} wwt below 8 m bls. Unfortunately, no bacterial cell numbers are available from groundwater from this sampling event.

Both sediment and groundwater samples exhibited maximum rates of substrate conversion at the uppermost sampling depths. Up to 1.9 mmol MUF-P were hydrolyzed by phosphatases per kilogram sediment (wwt) and hour in Liner 2 (Figure 4C). Turnover rates in Liner 1 reached maximum values of 1.2 mmol kg^{-1} wwt h^{-1} (Figure 4B). At 6.9 m bls, the activity started to level off at 180 μmol kg^{-1} wwt h^{-1} (Liner 2) and 60 μmol kg^{-1} wwt h^{-1} (Liner 1) on average. The gradient of MUF-P in groundwater samples was less pronounced and the activities were significantly lower, showing values of max. 32 nmol L^{-1} h^{-1} directly below the water table (Figure 4A), which corresponds to 10.9 nmol kg^{-1} h^{-1} wwt assuming a sediment porosity of 34%. Consequently, phosphatase activities in sediments were found up to six orders of magnitude higher than in groundwater. Sediment β-glucosidase activities were comparable

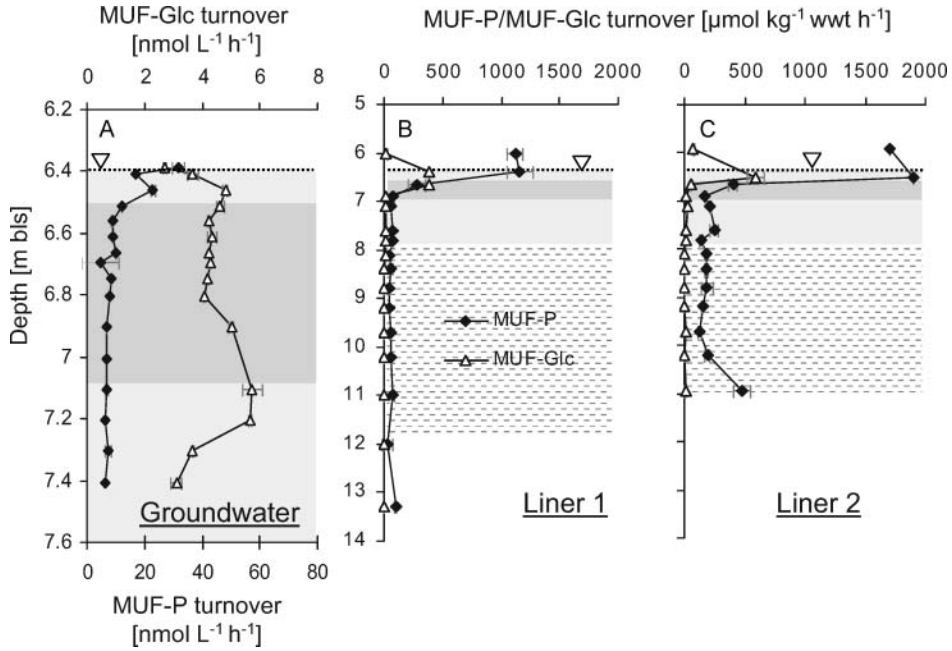

FIG. 4. Microbial enzyme activities in (A) groundwater and sediments of (B) Liner 1 and (C) Liner 2 in relation to BTEX (grey) and PAH (shaded) contaminated zones. values represent means of triplicate measurements ± SD.

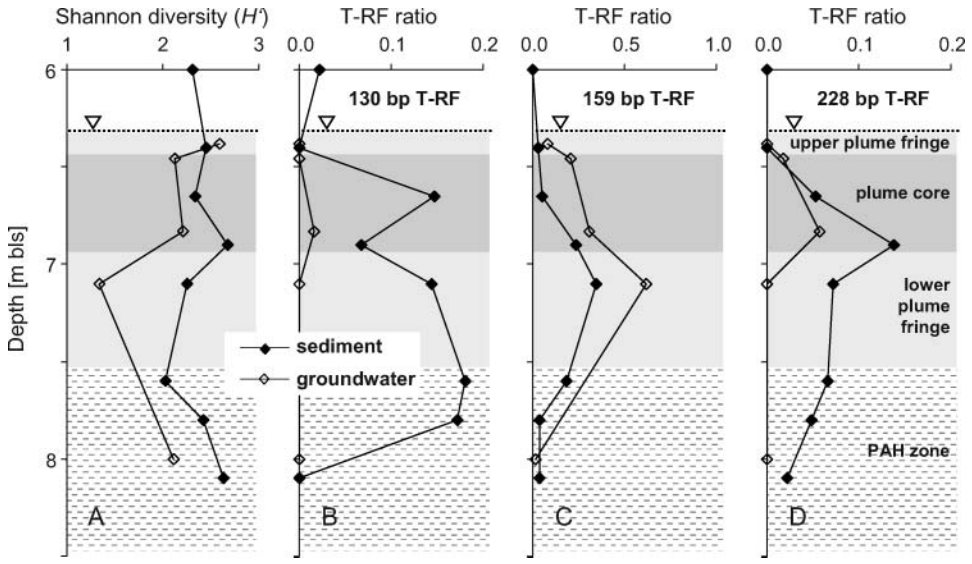

FIG. 5. Depth-distribution of (A) bacterial T-RFLP fingerprinting Shannon-Wiener diversity *H'* and relative T-RF abundance of characteristic T-RFs; i.e. related to (B) *Geobacter* spp. (130 bp), (C) *Desulfocapsa* spp. (159 bp), and (D) clostridial sulphate reducers and fermenters (228 bp) in sediments and corresponding groundwater samples of the Flingern site. The putative affiliation of the T-RFs is in accordance to previously published clone libraries from the same site (Winderl et al. 2008).

for both liners according to the individual depth zones (Figures 4B and C). Hydrolysis rates of MUF-Glc in groundwater exhibited slightly elevated values at the upper and lower fringe of the BTEX plume (Figure 4A). Similar to MUF-P turnover, sediment activities outreached groundwater activities by five orders of magnitude.

Depth-Resolved Analysis Bacterial Communities

T-RFLP analysis of bacterial communities indicated pronounced shifts in structure and diversity of total bacterial communities with depth (fingerprints are not shown). For groundwater, the Shannon-Wiener diversity *H'* as inferred from relative T-RF abundances was highest at the level of the capillary fringe/groundwater table and dropped to local minima within the lower plume fringe (7.1 m) (Figure 5A). For sediments, *H'* was very similar with depth, except at the lower part of the plume core, where a slightly increased local maximum of bacterial diversity was observed. A total of 77 distinct T-RFs was retrieved from both sediment and water samples, of which 21 peaks were unique for the sediment and 17 for the water samples. However, with the exception of the uppermost samples from near the capillary fringe, *H'* was always lower in water samples than in corresponding sediments.

To further elucidate these distinctions, we compared the depth-distribution of the relative abundance of selected T-RFs previously identified to represent important components of the degrader community. Respective results for sediment samples taken in 2005 revealed that especially the 130, 159, and 228 bp T-RFs represented dominating members of the contaminant-degrading bacterial community established in the lower plume fringe. As shown in a previous study by 16S rRNA gene cloning, these T-RFs were affiliated to microbes related to *Geobacter* spp., *Desulfocapsa* spp., and also clostridial sulphate reducers and fermenters (Winderl et al. 2008).

Albeit semi-quantitative, this assessment revealed pronounced distinctions in distribution patterns (Figure 5). T-RF abundances of over 15% were observed for 130 bp peaks (*Geobacter*-related microbes) in sediments of the plume core and over the lower plume fringe. In groundwater samples, however, this T-RF was only detected in one depth (6.83 m) and was thus almost not detectable over the entire depth transect (Figure 5B). In contrast, the 159 bp T-RF (*Desulfocapsa*-related) showed a very similar distribution with depth in both sample sets, with clear abundance maxima in the lower plume fringe at 7.1 m (Figure 5C). The 159 bp T-RF was always of a higher relative abundance in groundwater than in sediments (~62 vs. ~35%, respectively). Finally, the 228 bp T-RF (putatively representing clostridial sulphate reducers and fermenters) was present at a maximum frequency of ~14% and ~6% in both sediments and water of the lower plume core, respectively (Figure 5D).

To comparatively assess total bacterial community variance over depth in both sample sets, PCA statistics of the T-RFLP data set was conducted. The percentage of total community variability explained by the two primary PC factors inferred was no less than 59% (Figure 6). Surprisingly, data reduction indicated congruent community dynamics with depth over the different zones of the Flinger plume. As observed previously (Winderl et al. 2008), especially the populations of the lower fringe zone were resolved in ordination, indicating similar community patterns for both sediments and groundwater

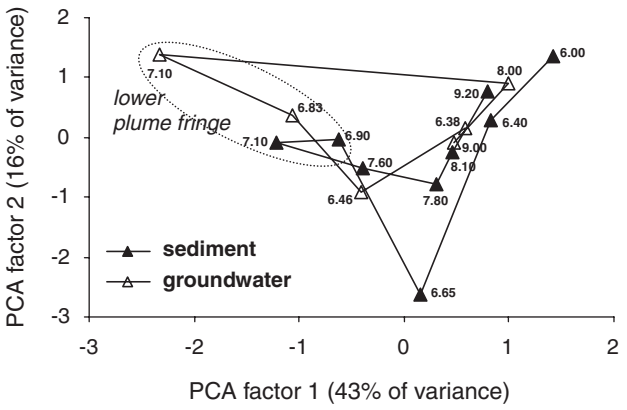

FIG. 6. Ordination of PCA factor scores for T-RFLP fingerprinting of sediment and water samples comprising the overall variance in depth-resolved bacterial community composition. The depths at which specific fingerprints were retrieved are indicated next to the ordination points.

samples in these depths. As observed before for the loading of PCA factors on specific T-RFs (Winderl et al. 2008), the distinction of the lower plume fringe degrader community was largely attributed to a high abundance of the 159 bp T-RF (factor loadings not shown). In summary, PCA illustrated similar community dynamics (clockwise shifts in virtual ordination) with depth for both sample sets, but dynamics (i.e., distinctions) with depth were more pronounced for groundwater samples (Figure 6).

DISCUSSION

Efficient biodegradation of organic contaminants in the subsurface requires two elements: (1) microbial populations with degradative capabilities, and (2) favourable geochemical and hydrological conditions (Haack and Bekins 2000). Then, *vice versa*, biodegradation processes are suggested to cause significant changes in groundwater and sediment properties, which include: (i) a rapid depletion of the energetically most favorable electron acceptors (i.e., oxygen and nitrate) (Anderson and Lovley 1997; Christensen et al. 2000), (ii) the appearance of metabolites and reaction products (e.g., reduced sulfur and iron species as shown in Figure 1, Figure 2), (iii) increase in pH and alkalinity owing to proton consumption during anaerobic oxidation of organic compounds (Table 1), and (iv) a decrease in redox potential as well as a change in specific conductivity due to the conversion of individual ions such as sulfate (Table 1) (Cozzarelli et al. 1999; Christensen et al. 2001). Some of these indicators may easily be followed in groundwater samples, however, some may clearly call for sediment data. For example, with respect to important redox processes (distribution of major electron acceptors and reaction products) information from groundwater samples is limited to dissolved chemical species. The role of solid electron acceptors such as ferric iron and the turnover of contaminants adsorbed to the sediment matrix can only be assessed directly in sediments, or indirectly via soluble metabolites and end products in groundwater. In contrast, major dissolved electron donors cannot be adequately monitored via sediment samples, and only partial information on intrinsic microbial communities and respective activities is obtainable from groundwater. As we discuss in the following, both, groundwater and sediments needs to be addressed when assessing NA potential in an organically polluted aquifer.

Small-Scale Physical-Chemical Heterogeneities in Groundwater and Sediments

Steep concentration gradients in groundwater clearly delineated a fine-scale vertical zonation of the BTEX plume. As obvious from Figure 1A, only the extraordinarily high-resolution of groundwater sampling allowed depicting the small-scale and steep geochemical gradients, which could not have been resolved by a conventional multi-level well with a vertical resolution of 0.5 to 1 m. However, groundwater samples did not provide comprehensive information regarding the PAH contamination. This is not surprising, as PAHs exhibit a high tendency to adsorb to the sediment matrix. In a recent study, Paisse et al. (2008) found up to 90% of PAHs sorbed and only a small fraction dissolved in groundwater. Naphthalene, due to its comparably low molecular weight and high solubility (Eberhardt and Grathwohl 2002), showed a similar distribution in groundwater as the monoaromatic hydrocarbons.

Compared to the maximally 16 mg L^{-1} of naphthalene dissolved in groundwater (= 5.4 mg per kg soil; Table 2), ~6- to 7-fold increased amounts were found sorbed to the sediments (Figures 2A and B). Sorption of PAHs to the sediment matrix is substantially influenced by the presence of organic matter, which is commonly regarded to be negligible in sandy aquifers, where mean organic carbon contents are in the range of only about 0.1% (Lovley and Chapelle 1995; Appelo and Postma 2005). Nevertheless, due to their hydrophobicity, the higher molecular weight PAHs acenaphthene and fluorene are strongly retained. In the Flingern aquifer, despite the

TABLE 2
Measured and calculated maximum concentrations of aromatic hydrocarbons in sediment and groundwater of the Flingern aquifer

Compound	Groundwater [mg L^{-1}][a]	Liner 2[b] Sediment Liner 1[b]	Liner 2[b] Sediment [mg kg^{-1}]	Calculated[c]
Toluene	45(15.3)	–	–	6.80
Naphthalene	16(5.4)	33.5	37	13.94
Acenaphthene	0.9(0.31)	6	1.6	4.11
Fluorene	0.7 (0.24)	26	32	5.07

[a]Parentheses indicate the corresponding sedimentary concentrations in mg $kg.^{-1}$

[b]Maximum concentrations measured in the respective sediment liners.

[c]Theoretically sorbed contaminant concentration calculated from max. contaminant concentrations measured in groundwater.

TABLE 3
Sorption properties and aqueous solubilities S_i of selected aromatic hydrocarbons

Compound	log K_{ow}	log K_{oc}	S_i at 25°C [mg L^{-1}][a]
Toluene	2.69[c]	2.18[d]	534.8
Naphthalene	3.36[b]	2.94[b]	31.7
Acenaphthene	3.98[c]	3.66[c]	3.93
Fluorene	4.18[c]	3.86[c]	1.98

S_i = aqueous solubility of organic compound i, K_{ow} = octanol-water coefficient, K_{oc} = organic carbon-water coefficient.
[a]Eberhardt and Grathwohl (2002).
[b]Appelo and Postma (2005).
[c]USACE (2002).
[d]Szabo et al. (1990).

relatively low soil organic carbon content of ∼0.3% (dry weight), concentrations of acenaphthene were 10- to 20-fold, fluorene concentrations even 100-fold higher in sediments than in groundwater.

The relation between adsorbed (C_s) and dissolved concentrations (C_w) can be expressed by the solid water distribution coefficient K_D of a given compound, according to

$$K_D = \frac{C_S[mg\,kg^{-1}]}{C_W[mg\,kg^{-1}]} \quad [1]$$

In soil–water systems, K_D is also defined by the product of the organic carbon–water distribution coefficient K_{oc} and the fraction f_{oc} of organic compounds in solution (Appelo and Postma 2005):

$$K_D = K_{oc} \times f_{oc} \quad [2]$$

Using literature K_{oc}values (Table 3) and measured f_{oc} (= 0.3%) and C_w in equations 1 and 2, the theoretically adsorbed contaminant concentration C_s can be calculated (Table 2). Measured concentrations of fluorene and naphthalene adsorbed to the sediment matrix exceeded calculated results by a factor of 5 and 2.5, respectively. Amounts of acenaphthene determined in the sediment agreed fairly well to theoretical values, overestimating the actual mean concentration by 10% (Table 2).

Calculated maximum toluene concentrations adsorbed to the sediment matrix amounted to ∼6.8 mg kg^{-1}, but neither toluene nor other BTEX compounds were detected in sediment samples of the Flingern site. Apparently, the sorption capacity of the sediment matrix for these substances was lower than expected. In conclusion, sediment samples alone would lead to inconclusive information on the BTEX contamination.

Considering the inaccuracies associated with the collection of sediments by liner coring, the differences in the distribution patterns of contaminants may also partly be ascribed to on site heterogeneities. "Hot spots" of pollutants and preferential flow paths in heterogeneous sediments may foster a diffuse spreading of contaminants. In the source zone, which is located ∼15 m upstream of the sampling area (Anneser et al. 2008a), the dense non-aqueous phase liquids (DNAPLs) are likely to seep down due to their higher density and molecular weight, which may explain the accumulation of PAHs in deeper zones in contrast to the lighter BTEX compounds.

Biodegradation via Sulfate Reduction

A significant enrichment of both ^{18}O and ^{34}S isotopes in groundwater sulfate proved microbial sulfate reduction to occur throughout the BTEX-contaminated zone, with pronounced activities across the lower plume fringe (Table 1; see also Anneser et al. (2008a)). Inverse gradients of dissolved sulfate and sulfide (Figure 1B), which are regarded as indicators of ongoing sulfate reduction, support this hypothesis. Further geochemical evidence for bacterial sulfate reduction derived from a distinct peak of reduced inorganic sulfur extracted from sediment samples, which again hints at high sulfate reduction activity at 7.1 m bls, marking the transition between heavily and less contaminated groundwater in the lower plume fringe (Figure 2C). The lack of sulfide at the upper plume fringe is most likely attributed to scavenging of sulfide by both complexation and reoxidation reactions with Fe(II) (Stumm and Morgan 1996; Cozzarelli et al. 1999; Kostka et al. 2002).

Iron Reduction and Iron Cycling Processes

Iron reduction has previously been shown to occur at the Flingern site (Eckert 2001). Groundwater analysis revealed iron reducing activity being most pronounced at the upper and lower plume fringe (Eckert 2001; Anneser et al. 2008a). Elevated concentrations of dissolved Fe(II) measured in groundwater samples hint at significant iron reduction in the upper 20 cm of the saturated zone (Figure 1C). However, only sediment analysis could show that considerable amounts of readily extractable ferric iron are actually present in this zone (data not shown). At the interface between the unsaturated and saturated zone, cycling of iron species is likely to proceed at high rates. Transient hydraulic conditions causing a fluctuating groundwater table govern regular periods of re-oxidation and reduction, providing a regeneration of sedimentary electron acceptors (Ulrich et al. 1998, 2003). A minor secondary peak of ferrous iron in groundwater was observed at the lower plume fringe. This pattern has already been observed in previous investigations at that site (Anneser et al. 2008a, 2008b).

From a thermodynamic point of view, iron reduction is considered to be energetically more favorable than sulfate reduction (Lovley and Chapelle 1995). Nevertheless, bacterial iron reduction in organically contaminated porous aquifers is frequently limited by the availability of Fe(III) species (Albrechtsen and Christensen 1994; Tucillo et al. 1999). In the sediments of Liner 1 and 2, extractable ferric iron did only exceptionally account for more than 1 g kg^{-1} wwt. Crystalline Fe(III) species, on

the other hand, were available at two to fourfold higher concentrations all across the anoxic aquifer section, with maxima above and below the BTEX plume (data not shown). Although bacteria are theoretically capable of using crystalline Fe(III) as electron acceptor (Roden and Zachara 1996), it is only slowly converted and less attractive to microorganisms owing to their stability and inaccessibility (Lovley 2001).

It has to be considered, furthermore, that only a small ratio of the ferrous iron is found dissolved in groundwater, while the major part remains associated with sediment surfaces. This can further decrease the availability of sedimentary Fe(III) to attached bacteria. Interestingly, readily extractable ferrous iron in sediments exhibited highest values (3–4 g kg^{-1} wwt) below the BTEX plume (Figure 2D). Sediment data thus points at an undepleted reservoir of ferric iron in deeper zones of the aquifer. Independent from depth the amount of Fe(II) associated with the sediment in the saturated zone accounted for >99%, while less than 1% was found dissolved in groundwater. A similar distribution of Fe (II) between groundwater and sediment matrix was also reported for other aquifers (Lovley and Phillips 1988; Heron et al. 1994). Elevated concentrations of Fe(II) and concurrent low sulfide concentrations, as found near the capillary fringe, point also at sulfide oxidation with ferric iron, a topic which needs further investigations.

Microbial Patterns in Groundwater and Sediments

It has repeatedly been shown that cells attached to surfaces can account for 90 to 99.99% of the microbial biomass in porous aquifers (Griebler and Lueders 2009). The sediment cell counts, therefore, matched well general findings. However, the two biomass peaks in Liner 1 and 2 (here the lower one was less pronounced) impressively mirrored zones of highest biodegradation activities as indicated by redox gradients. Unfortunately, no data on the number of suspended cells were available for the February 2006 sampling campaign due to accidental loss of sample vials.

Thus no direct sediment-groundwater comparisons could be performed for this particular parameter. However, the sediment data obtained may be well compared with groundwater data from a sampling campaign 6 months later (Anneser et al. 2008a). The general distribution of bacteria in groundwater was highly similar to the sediment pattern reported here. In detail, the total number of cells was highest in the uppermost sampling point in the upper plume fringe zone, exhibiting 1.2×10^6 cells mL^{-1}. In the plume core, cell numbers were ten times less with an average value of 2.1×10^5 mL^{-1}, but increased again to 5×10^5 mL^{-1}at the lower plume fringe. Further down, a slight decrease of cell numbers to 3.2×10^5 mL^{-1} was observed, interrupted by another distinct peak (6.8×10^5 mL^{-1}) right in the area of highest PAH concentrations in the sediment (Anneser et al. 2008a). Comparing total cell counts in groundwater and sediments on a volume basis (assuming a sediment active porosity of 34%) revealed between 97.7 and 99.8% of the cells attached to the sediments. Similar values are reported from an aquifer at a landfill site, where 98.3% of the cells were found attached (Röling et al. 2001). Also (Brad et al. 2008) emphasized the ecological role of sediments, which harbored cell numbers approximately one magnitude higher compared to groundwater.

Assuming a sediment surface area of 22 (coarse sand) to 450 cm^2 g^{-1} (fine sand) (Leichtfried 1985; Albrechtsen and Christensen 1994) and a mean area of 0.5 μm^2 covered by a typical bacterial cell in groundwater (Griebler et al. 2002), 4.4×10^9 to 9×10^{10} attached cells g^{-1} would be required to form a closed unicellular biofilm. In fact, the highest bacterial abundance determined from our sediment samples, i.e., at the lower plume fringe in Liner 1 (Figure 3), accounts for a surface coverage of only 0.08 to 1.6%. This colonization density is comparable with other studies in aquifers (Griebler et al. 2001, 2002) and marine sands (Weise and Rheinheimer 1978; Yamamoto and Lopez 1985). In such a case it is questionable, however, whether the term 'biofilm' is appropriate or whether we should rather refer to single cells and microcolonies.

On the other hand, the maximal total direct cell counts of 4.1 to 4.8×10^7 cells g^{-1} wwt reported here for the upper sediment layers account for only ~20% of the maximally 2.4×10^8 bacterial 16S rRNA genes g^{-1} wwt detected via qPCR in similar depths upon sediment sampling in 2005 (Winderl et al. 2008). This number, consequently, would result in a surface coverage of 0.3 to 5.5%. It is likely that both quantification methods carry intrinsic biases, thus although they may be well suited to compare microbial distributions over depth, any absolute interpretations in terms of sediment carrying capacities should be treated with caution.

Indeed, the total cellular distribution did not reveal much about microbial activities and ongoing biodegradation processes. Hydrolysis rates of extracellular phosphatases (MUF-P substrate) and glucosidases (MUF-Glc substrate) (Freeman et al. 1995) revealed microbial activities 5–6 orders of magnitude higher in sediments compared to groundwater (Figure 4). Again, highest values were obtained from the interface between the unsaturated and saturated zone, i.e., the capillary zone and upper plume fringe. As alkaline phosphatases are subject to catabolite repression by their product phosphate (Coolen and Overmann 2000), the high phosphatase activity in this zone corresponds well with the local decrease in phosphate concentration.

Recycling of electron acceptors and mixing with electron donors from the contaminated area make the capillary fringe a favorable place for biodegradation (Sinke et al. 1998; Ronen et al. 2000). Higher activities of attached vs. suspended communities have been shown in a number of studies (Holm 1992; Madsen and Ghiorse 1993; Albrechtsen and Christensen 1994; Lehman and O'Connell 2002). However, with β-glucosidase activity Lehman et al. (2002) also found the opposite pattern. Concluding, when comparing the gradients in Figure 3 and Figure 4 it can be seen that zones of enhanced microbial

activity matched well zones with highest biomass concentration. High biomass zones in contaminated aquifers may thus be a good proxy for zones of pronounced NA activities.

Bacterial Community Shifts in Sediment and Water

Shifts in bacterial community composition over a depth transect of the Flingern BTEX-plume have been observed before for sediment samples taken in June 2005 (Winderl et al. 2008). Hence, an apparently highly specialized degrader population dominated by deltaproteobacterial and clostridal iron reducers, sulfate reducers and fermenters was found to dominate the lower plume fringe. In the present study, we repeated these analyses for selected sediment depths sampled in February 2006, but, more importantly, aimed to compare sedimentary community fingerprints to those obtained from corresponding groundwater samples. Depth-resolved fingerprinting of bacterial communities in water and sediments revealed that only ∼50% of all detected T-RFs were shared between water and sediment samples. This is evidence that even if very close corresponding depths are sampled, the two compartments are partially separated on the microscale, and that not all aquifer microbes are equally detectable in both.

This comparison may provide valuable insights on the ecology of the different microbes, as exemplified, e.g., by the comparative distribution pattern of the *Geobacter*-related T-RF (130 bp). This T-RF was practically not detected in groundwater, which may be attributed to the preference of these microbes to insoluble electron acceptors such as ferric iron and elemental sulfur, and hence to a lifestyle attached to mineral surfaces (Weber et al. 2006). In contrast, other microbes putatively more dependent on dissolved electron acceptors, such as the *Desulfocapsa*-relatives represented by the 159 bp T-RF, were consistently distributed with depth in both sediment and water samples, but always detected in higher ratios in groundwater. Moreover, the maximal abundance of this T-RF was surprisingly congruent to the peak of sulfide (Figure 1B). This may be an indication that the distribution of these specific microbes is clearly correlated to the localization of sulfate reducing processes within the Flingern aquifer. We are fully aware that the inference of peak abundances in T-RFLP fingerprinting allow only for a semi-quantitative assessment of community composition and provide no absolute abundances of specific populations (Lueders and Friedrich 2003; Thies 2007; Hartmann and Widmer 2008). Nevertheless, we are confident to demonstrate important distinctions, but also similarities in depth-resolved microbial community distribution in sediments and water at the site using this approach. A significant correlation between community structure and degree of contamination was also observed in sediments of a leachate-impacted aquifer (Brad et al. 2008).

Over depth, the non-shared T-RFs appeared mainly in the deeper PAH zone (56% of all singletons). Thus, the upper zones dominated by the BTEX plume seem to impose much stronger selective pressures on the microorganisms, leading to a more uniform appearance of bacteria in both compartments. This was also reflected in the congruent depth-related bacterial community shifts identified in PCA, which supports both strategies to provide relevant information on depth-resolved microbial distribution patterns.

Up to now, researchers have been well aware that only a minor fraction of total aquifer microbiota are found in groundwater itself (Alfreider et al. 1997; Lehman et al. 2001; Griebler et al. 2002). Although we do not provide a direct quantitative comparison of microbial abundance in groundwater and sediments for the same sampling date, this is to our knowledge the first systematic evaluation of the congruence of physical-chemical and microbial community patterns found in both compartments. We show that major microbial community indicators such as total diversity or the relative abundance of selected community members are distributed in similar, however not identical patterns. Sediment samples always seem to comprise most genetic information found also in the water, but this relation is not correct *vice versa*. Nevertheless, as ∼50% of all T-RF peaks were shared between both compartments, both strategies can be considered appropriate to detect spatial and temporal distinctions in the microbial community composition at contaminated sites.

In summary, the data presented in this study emphasize the importance of considering both groundwater and sediment parameters for assessing natural attenuation potential and activities at organically contaminated aquifers. Unlike groundwater samples, which provide only a momentary snapshot of dissolved reactants and dependant microbes *in situ*, sediment analyses allowed more profound insights into the history of the aquifer and into long-term processes occurring at a site, not only in the aquatic, but also the sedimentary compartments.

REFERENCES

Albrechtsen H-J, Winding A. 1992. Microbial biomass and activity in subsurface sediments from Vejen, Denmark. Microb Ecol 23:303.

Albrechtsen HJ, Christensen TH. 1994. Evidence for microbial iron reduction in a landfill leachate-polluted aquifer (Vejen, Denmark). Appl Environ Microbiol 60:3920–3925.

Alfreider A, Krössbacher M, Psenner R. 1997. Groundwater samples do not reflect bacterial densities and activity in subsurface systems. Water Res 31:832–840.

Anderson RT, Lovley DR. 1997. Ecology and biogeochemistry of in situ groundwater bioremediation. Adv Microb Ecol 15:289–350.

Anneser B, Richters L, Griebler C. 2008b. Application of high-resolution groundwater sampling in a tar oil–contaminated sandy aquifer. Studies on small-scale abiotic gradients. In Advances in subsurface pollution of porous media: indicators, processes and modelling. Candela L, Vadillo I, Elorza FJ. (eds.). Leiden, NL:CRC Press/Balkema. P 107–122.

Anneser B, Einsiedl F, Meckenstock RU, Richters L, Wisotzky F, Griebler C. 2008a. High-resolution monitoring of biogeochemical gradients in a tar oil-contaminated aquifer. Appl Geochem 23:1715–1730.

Appelo CAJ, Postma D. 2005. Geochemistry, Groundwater and Pollution. Leiden, The Netherlands: Taylor & Francis Group plc.

Bamforth SM, Singleton I. 2005. Bioremediation of polycyclic aromatic hydrocarbons: current knowledge and future directions. J Chem Technol Biotechnol 80:723–736.

Bekins, BA, Cozzarelli IM, Godsy EM, Warren E, Essaid HI, and Tuccillo ME 2001. Progression of natural attenuation processes at a crude oil spill site: II.

Controls on spatial distribution of microbial populations. J Contam Hydrol 53:387–406.

Brad T, van Breukelen BM, Braster M, van Straalen NM, Roling WF. 2008. Spatial heterogeneity in sediment-associated bacterial and eukaryotic communities in a landfill leachate-contaminated aquifer. FEMS Microbiol Ecol.

Brielmann H, Griebler C, Schmidt SI, Michel R, Lueders T. 2009. Effects of thermal energy discharge on shallow groundwater ecosystems. FEMS Microbiol Ecol 68:273–286.

Christensen TH, Bjerg PL, Banwart SA, Jakobsen R, Heron G, Albrechtsen H-J. 2000. Characterization of redox conditions in groundwater contaminant plumes. J Contam Hydrol 45:165–241.

Christensen TH, Kjeldsen P, Bjerg PL, Jensen DL, Christensen JB, Baun A, et al. 2001. Biogeochemistry of landfill leachate plumes. Appl Geochem 16:659–718.

Coolen MJL, Overmann J. 2000. Functional exoenzymes as indicators of metabolically active bacteria in 124,000-year-old sapropel layers of the eastern mediterranean sea. Appl Environ Microbiol 66:2589–2598.

Cozzarelli IM, Herman JS, Baedecker MJ, Fischer JM. 1999. Geochemical heterogeneity of a gasoline-contaminated aquifer. J Contam Hydrol 40:261–284.

Eberhardt C, Grathwohl P. 2002. Time scales of organic contaminant dissolution from complex source zones: coal tar pools vs. blobs. J Contam Hydrol 59:45–66.

Eckert, P. 2001. Untersuchungen zur Wirksamkeit und Stimulation natürlicher Abbauprozesse in einem mit gaswerksspezifischen Schadstoffen kontaminierten Grundwasserleiter. In Bochumer Geologische und Geotechnische Arbeiten. Bochum: PhD thesis, Ruhr-Universität Bochum, Germany. P 123.

Freeman C, Liska G, Ostle NJ, Jones SE, Lock MA. 1995. The use of fluorogenic substrates for measuring enzyme activity in peatlands. Plant Soil 175:147–152.

Griebler C, Lueders T. 2009. Microbial diversity in groundwater ecosystems. Freshwater Biol 54:649–677.

Griebler C, Mindl B, Slezak D. 2001. Combining DAPI and SYBR Green II for the enumeration of total bacterial numbers in aquatic sediments. Int Rev Hydrobiol 86:453–465.

Griebler C, Mindl B, Slezak D, Geiger-Kaiser, M. 2002. Distribution patterns of attached and suspended bacteria in pristine and contaminated shallow aquifers studied with an in situ sediment exposure microcosm. Aquat Microb Ecol 28:117–129.

Haack SK, Bekins BA. 2000. Microbial populations in contaminant plumes. Hydrogeol J 8:63–76.

Hartmann M, Widmer F. 2008. Reliability for detecting composition and changes of microbial communities by T-RFLP genetic profiling. FEMS Microbiol Ecol 63:249–260.

Hazen TC, Jimenez L, Lopez de Victoria G, Fliermans CB. 1991. Comparison of bacteria from deep subsurface sediments and adjacent groundwater. Microb Ecol 22:293–304.

Hendel B, Marxsen J. 1997. Measurement of low-level extracellular enzyme activity in natural waters using fluorigenic model substrates. Acta Hydrochim Hydrobiol 25:253–258.

Heron G, Crouzet C, Bourg ACM, Christensen TH. 1994. Speciation of Fe(I I) and Fe(I I I) in contaminated aquifer sediments using chemical extraction techniques. Environ Sci Technol 28:1698–1705.

Holm NG. 1992. Origins of Life. Dordrecht, Netherlands.

Kao CM, Kota S, Ress B, Barlaz MA, Borden RC. 2001. Effects of subsurface heterogeneity on natural bioremediation at a gasoline spill site. Water Sci Technol 43:341—348.

Kölbel-Boelke J, Hirsch P. 1989. Comparative physiology of biofilm and suspended microorganisms in the groundwater environment. In Structure and Function of Biofilms. Characklis WG, Wilderer PA. (eds.). Chichester: John Wiley. P 221–238.

Kostka JE, Roychoudhury A, Van Cappellen P. 2002. Rates and controls of anaerobic microbial respiration across spatial and temporal gradients in saltmarsh sediments. Biogeochemistry 60:49–76.

Lehman RM, O'Connell SP. 2002. Comparison of extracellular enzyme activities and community composition of attached and free-living bacteria in porous medium columns. Appl Environ Microbiol 68:1569–1575.

Lehman RM, Colwell FS, Bala GA. 2001. Attached and unattached microbial communities in a simulated basalt aquifer under fracture- and porous-flow conditions. Appl Environ Microbiol 67:27992809.

Leichtfried M. 1985. Organic matter in gravel streams (Project Ritrodat-Lunz). Verh Int Ver Limnol 22:2058–2062.

Lindahl V, Bakken LR. 1995. Evaluation of methods for extraction of bacteria from soil. FEMS Microbiol Ecol 16:135–142.

Lovley DR. 2001. Anaerobes to the rescue. Science 293:1444–1446.

Lovley DR, Phillips EJ. 1987. Rapid assay for microbially reducible ferric iron in aquatic sediments. Appl Environ Microbiol 53:1536–1540.

Lovley DR, Phillips EJ. 1988. Novel mode of microbial energy metabolism: organic carbon oxidation coupled to dissimilatory reduction of iron or manganese. Appl Environ Microbiol 54:1472–1480.

Lovley DR, Chapelle FH. 1995. Deep subsurface microbial processes. Rev Geophys 33:365–381.

Lueders T, Friedrich MW. 2002. Effects of amendment with ferrihydrite and gypsum on the structure and activity of methanogenic populations in rice field soil. Appl Environ Microbiol 68:2484–2494.

Lueders T, Friedrich MW. 2003. Evaluation of PCR amplification bias by terminal restriction fragment length polymorphism analysis of small-subunit rRNA and mcrA genes by using defined template mixtures of methanogenic pure cultures and soil DNA extracts. Appl Environ Microbiol 69:320–326.

Madsen EL, Ghiorse WC. 1993. Groundwater microbiology: subsurface ecosystem processes. In Aquatic Microbiology–An Ecological Approach. Blackwell Scientific Publications. P167–213.

McGuire JT, Smith EW, Long DT, Hyndman DW, Haack SK, Klug MJ, Velbel MA. (2000) Temporal variations in parameters reflecting terminal-electron-accepting processes in an aquifer contaminated with waste fuel and chlorinated solvents. Chem Geol 169:471–485.

Nebe-von-Caron G, Stephens PJ, Hewitt CJ, Powell JR, Badley RA. 2000. Analysis of bacterial function by multi-colour fluorescence flow cytometry and single cell sorting. J Microbiol Meth 42:97–114.

Paisse S, Coulon F, Goni-Urriza M, Peperzak L, McGenity TJ, Duran R. 2008. Structure of bacterial communities along a hydrocarbon contamination gradient in a coastal sediment. FEMS Microbiol Ecol 66:295–305.

Roden EE, Zachara JM. 1996. Microbial reduction of crystalline iron(III) oxides: influence of oxide surface area and potential for cell growth. Environ Sci Technol 30:1618–1628.

Röling WF, van Breukelen BM, Braster M, Lin B, van Verseveld HW. 2001. Relationships between microbial community structure and hydrochemistry in a landfill leachate-polluted aquifer. Appl Environ Microbiol 67:4619–4629.

Ronen D, Scher H, Blunt M. 2000. Field observations of a capillary fringe before and after a rainy season. J Contam Hydrol 44:103–118.

Sinke AJC, Dury O, Zobrinst J. 1998. Effects of a fluctuating water table: column study on redox dynamics and fate of some organic pollutants. J Contam Hydrol 33:231–246.

Stumm W, Morgan JJ. 1996. Aquatic Chemistry: John Wiley & Sons Inc, New York.

Szabo G, Prosser SL, Bulman RA. 1990. Determination of the adsorption coefficient Koc of some aromatics for soils by RP-HPLC on two immobilized humic acid phases. Chemosphere 21:777–788.

Thies JE. 2007. Soil microbial community analysis using terminal restriction fragment length polymorphisms. Soil Sci Soc Am J 71:579–591.

Tucillo ME, Cozzarelli IM, Herman JS. 1999. Iron reduction in the sediments of a hydrocarbon-contaminated aquifer. Appl Geochem 14:655–667.

Ulrich GA, Krumholz LR, Suflita JM. 1997. A rapid and simple method for estimating sulfate reduction activity and quantifying inorganic sulfides. Appl Environ Microbiol 63:4626.

Ulrich GA, Breit GN, Cozzarelli IM, Suflita JM. 2003. Sources of sulfate supporting anaerobic metabolism in a contaminated aquifer. Environ Sci Technol 37:1093–1099.

Ulrich GA, Martino D, Burger K, Routh J, Grossman EL, Ammerman JW, Suflita JM. 1998. Sulfur cycling in the terrestrial subsurface: commensal interactions, spatial scales, and microbial heterogeneity. Microb Ecol 36:141–151.

USACE. 2002. Soil vapor extraction and bioventing. In Engineering and Design Washington, DC: US Army Corps of Engineers.

Weber KA, Achenbach LA, Coates JD. 2006. Microorganisms pumping iron: anaerobic microbial iron oxidation and reduction. Nat Rev Microbiol 4:752–764.

Weise W, Rheinheimer G. 1978. Scanning electron microscopy and epifluorescence investigation of bacterial colonization of marine sand sediments. Microb Ecol 4:175–188.

Widdel F, Bak F. 1992. Gram negative mesophilic sulfate reducing bacteria. In The Prokaryotes. A Handbook on the Biology of Bacteria: Ecophysiology, Isolation, Identification, and Applications. Balows HGTA, Dwarkin M, Harder W, Schleifer KH. (eds.). Springer, New York. P 3352–3378.

Winderl C, Anneser B, Griebler C, Meckenstock RU, Lueders T. 2008. Depth-resolved quantification of anaerobic toluene degraders and aquifer microbial community patterns in distinct redox zones of a tar oil contaminant plume. Appl Environ Microbiol 74:792–801.

Yamamoto N, Lopez G. 1985. Bacterial abundance in relation to surface area and organic content of marine sediments. L Exp Mar Biol Ecol 90:209–220.

Zhou J, Bruns MA, Tiedje JM. 1996. DNA recovery from soils of diverse composition. Appl Environ Microbiol 62:316–322.